Available online at www.sciencedirect.com
ScienceDirect
Journal of the European Ceramic Society 31 (2011) 1597–1602
www.elsevier.com/locate/jeurceramsoc

Two-step pressure sintering of transparent lutetium oxide by spark plasma sintering

Liqiong An [a,b], Akihiko Ito [a], Takashi Goto [a,*]

[a] *Institute for Materials Research, Tohoku University, Sendai 980-8577, Japan*
[b] *Research Fellow of the Japan Society for the Promotion of Science, Japan*

Received 6 December 2010; received in revised form 28 February 2011; accepted 7 March 2011
Available online 14 April 2011

Abstract

Transparent lutetium oxide (Lu_2O_3) body was prepared by spark plasma sintering using a two-step pressure profile combined with a low heating rate. The effects of pre-load pressures from 10 to 100 MPa and heating rates from 0.03 to 1.67 K s^{-1} on the microstructures and optical properties were investigated. With increasing pre-load pressures from 10 to 100 MPa, the grains became smaller with a narrower distribution, whereas the transmittance showed maxima at 30 MPa. The average grain size slightly increased from 0.67 to 0.86 μm as the heating rate increased from 0.03 to 1.67 K s^{-1}, while the transmittance decreased. Transmittances of 60% at 550 nm and 79% at 2000 nm were obtained under a pre-load pressure of 30 MPa at a heating rate of 0.17 K s^{-1}.

Keywords: Lutetium oxide; Lu_2O_3; Transparent; Spark plasma sintering

1. Introduction

Spark plasma sintering (SPS) allows for the compaction of ceramics and metals to a dense body in a short time, commonly within a few minutes.[1] The densification process in SPS is generally divided into three stages. The first stage is characterized by the packing of the particles, the second stage is related to a diffusion process accompanying the neck formation and grain sliding, and the final stage is the removal of pores mainly through the grain boundary. An applied pressure strongly affects the initial packing and densification in the second and third stages. A high pressure is constantly applied in the common SPS process. Recently, highly transparent ceramics with controlled microstructures have been prepared by a two-step pressure profile, i.e., a low pre-loading pressure at low temperatures and a high pressure at high temperatures.[2] The heating rate is another important sintering parameter for densification in the second and third stages. Although a fast heating rate of over 1.67 K s^{-1} is widely used in SPS, a low heating rate was applied to fabricate highly transparent Al_2O_3[3] and $MgAl_2O_4$.[4] The combination of the two-step profile and low heating rate can be more advantageous to obtain fine microstructure bodies with improved transparencies.

Rare earth sesquioxides, such as Y_2O_3, Lu_2O_3 and Sc_2O_3, are promising laser host materials for high-power and ultrashort pulse lasers. In particular, Lu_2O_3 provides the highest doping concentration for Yb^{3+} while maintaining high heat conductivity due to the similar mass and ionic radius of Lu^{3+} and Yb^{3+}. Although single crystal growth is a common technique to prepare transparent materials, the melting point of Lu_2O_3 (2763 K) is too high.[5] We first prepared a dense and transparent Lu_2O_3 body by SPS using commercial powders.[6] To improve transparency of the Lu_2O_3 body, we applied a two-step pressure profile combined with a low heating rate. In this paper, the effects of pre-load pressure on the two-step pressure profile and the heating rate of SPS on the microstructure and transmittance of the Lu_2O_3 body were investigated.

2. Experimental procedure

Lu_2O_3 commercial powder (purity: 99.9%; 50 nm in average diameter, Kojundo Chemical, Japan) was sintered using an SPS apparatus (SPS-210 LX, SPS SYNTEX, Japan) in a vacuum. As-received powder was poured into a graphite die having an inner

* Corresponding author.
E-mail address: goto@imr.tohoku.ac.jp (T. Goto).

0955-2219/$ – see front matter © 2011 Elsevier Ltd. All rights reserved.
doi:10.1016/j.jeurceramsoc.2011.03.014

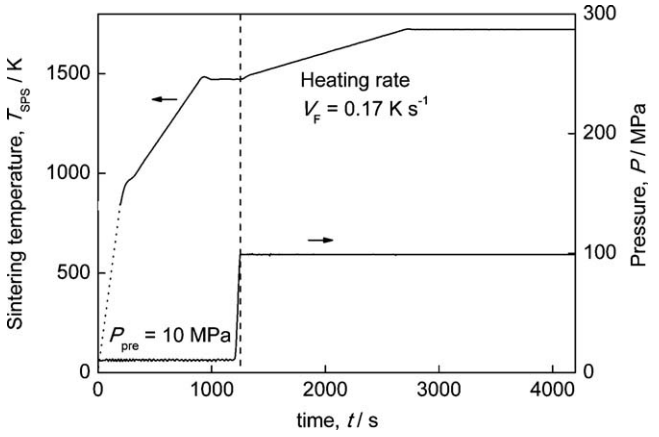

Fig. 1. Typical heating profile and pressure application regime as a function of the time t at $P_{pre} = 10$ MPa and $V_F = 0.17$ K s^{-1}. Dashed line refers to the application of final pressure of 100 MPa.

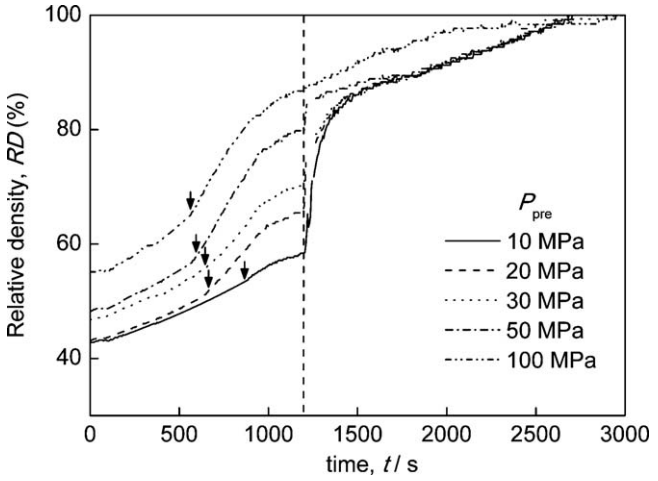

Fig. 2. Sintering curves of Lu_2O_3 bodies sintered at $P_{pre} = 10$–100 MPa and $V_F = 0.17$ K s^{-1}. Arrows indicate the starting of densification enhancement. Dashed line refers to the application of final pressure.

diameter of 10 mm. The graphite die was covered with a thermal insulator carbon fiber. An optical pyrometer was used to measure the temperature of the graphite die surface. The temperature was first increased to 873 K within 180 s and then increased to 1473 K within 720 s and held for 300 s. The temperature was further increased from 1473 to 1723 K at different heating rates (V_F) between 0.03 and 1.67 K s^{-1}. The final sintering temperature was 1723 K and was held for 2.7 ks. The pressure was applied in two steps. Uniaxial pressures ranging from 10 to 100 MPa were pre-loaded (P_{pre}) at room temperature. The pressure was further increased to the final pressure of 100 MPa within 60 s when the temperature was increased from 1473 to 1723 K. Fig. 1 shows a typical temperature and pressure profile as a function of time (t) at $P_{pre} = 10$ MPa and $V_F = 0.17$ K s^{-1}. The shrinkage of the specimens was continuously monitored by the displacement of the punch rod. The spark-plasma-sintered specimens were mirror-polished on both sides using diamond slurry. The thickness of the specimens was approximately 1 mm.

The density was measured by the Archimedes method in distilled water. All the specimens had relative densities greater than 99.5%. The sintered bodies were thermally etched at 1573 K in air for 3.6 ks. The microstructure was observed by a field-emission scanning electron microscope (FESEM, JSM-7500F, JEOL, Japan). The average grain size was determined by the linear intercept length of the grains in the FESEM images, multiplied by the statistical factor 1.56.[7] The inline transmittances in the visible and infrared ranges were measured using a

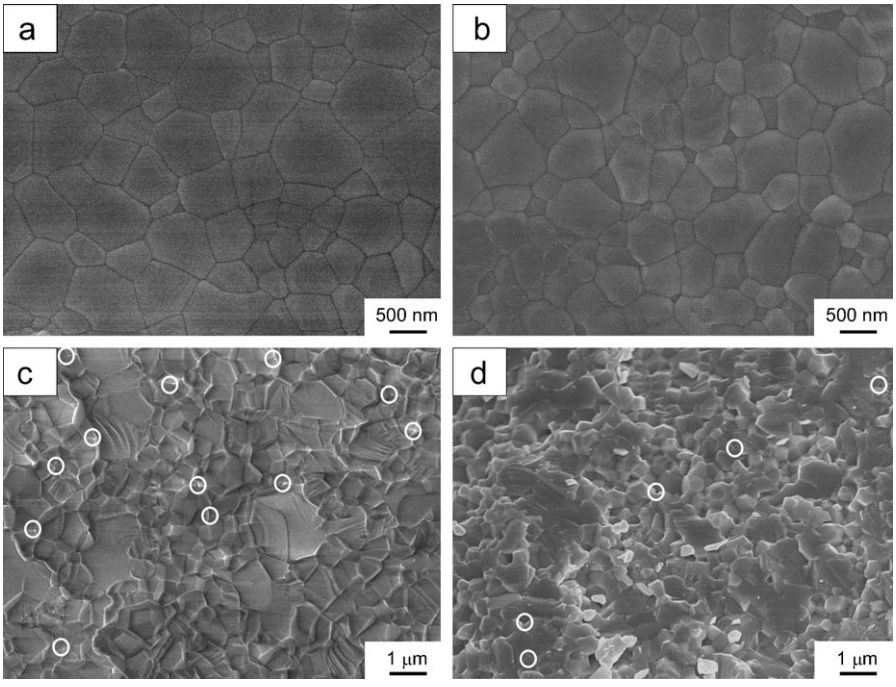

Fig. 3. FESEM images of thermally etched and fracture surfaces of Lu_2O_3 bodies sintered at P_{pre} = (a, c) 10 and (b, d) 100 MPa and $V_F = 0.17$ K s^{-1}. White circles denote pores.

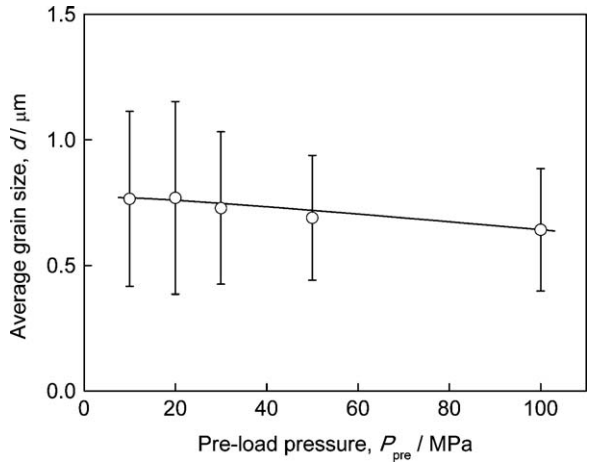

Fig. 4. Effect of P_{pre} on the average grain size of Lu_2O_3 bodies at $V_F = 0.17\ K\ s^{-1}$.

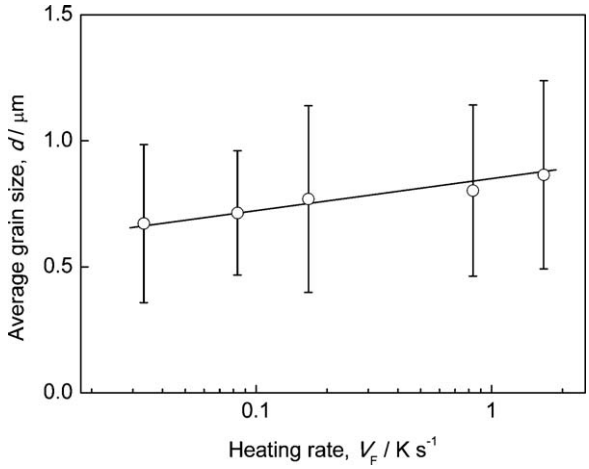

Fig. 7. Effect of V_F on the average grain size of Lu_2O_3 bodies at $P_{pre} = 10$ MPa.

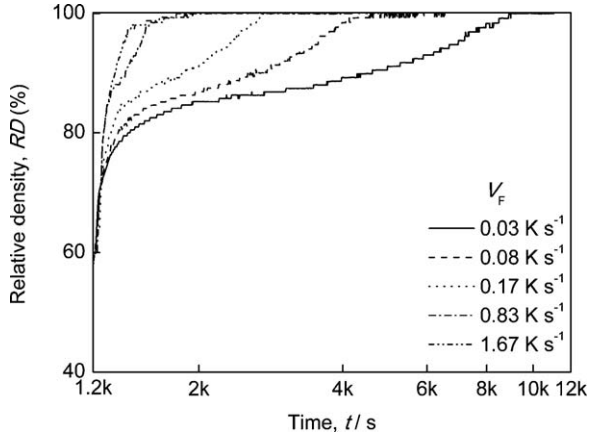

Fig. 5. Sintering curves of Lu_2O_3 bodies sintered at $P_{pre} = 10$ MPa and $V_F = 0.03$–$1.67\ K\ s^{-1}$.

spectrophotometer (UV-3101PC, Shimadzu, Japan) in the wavelength range from 190 to 2500 nm.

3. Results and discussion

3.1. Effects of the pre-load pressure

Fig. 2 shows the sintering curves of the Lu_2O_3 bodies at $P_{pre} = 10$ to 100 MPa and $V_F = 0.17\ K\ s^{-1}$. The initial packing density (at $t = 0$) increased from 42% to 55% as P_{pre} was increased from 10 to 100 MPa. Densification was enhanced between $t = 560$ and 890 s (arrows in Fig. 2). It was observed that the higher the P_{pre}, the earlier the start time of the densification enhancement. When the applied pressure increased from P_{pre} to 100 MPa (dashed line in Fig. 2), the relative density significantly increased. This effect was more pronounced at a lower P_{pre}. The sintering curves almost coincided after $t = 1750$ s at $P_{pre} \leq 50$ MPa where a two-step pressure profile was used. The sintering curve was almost continuous at $P_{pre} = 100$ MPa because the applied pressure was constant throughout the entire process.

It is generally understood that applied pressure can directly affect particle rearrangement, destroying agglomerations and resulting in an increase in the compaction of particles in the first sintering stage. Moreover, a high applied pressure can cause rapid densification by plastic deformation and particle sliding in the second sintering stage.[8] In the present study, P_{pre} affected not only the initial packing but also the start time of the densification enhancement indicated by the arrows in Fig. 2. Ehre et al. also reported that the volume shrinkage of MgO by hot pressing began at room temperature at 150 MPa, while no shrinkage was observed at 50 MPa until 673 K.[9] After the pressure increased to 100 MPa, the relative density gradually reached above 90% with increasing t and sintering temperature. Densification in the final stage might be mainly due to grain boundary diffusion

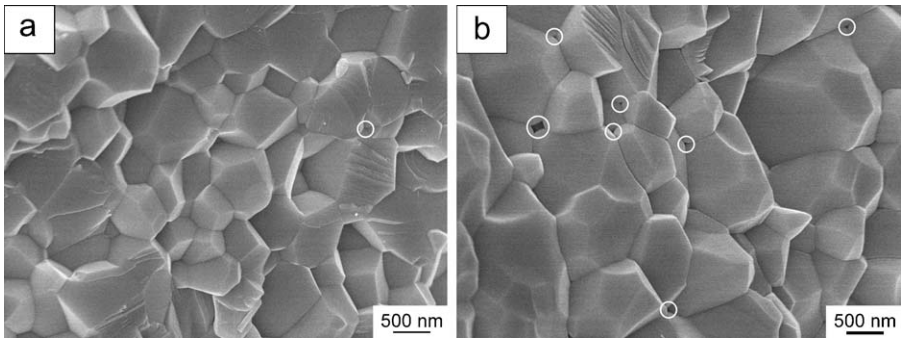

Fig. 6. FESEM images of fracture surfaces of Lu_2O_3 bodies sintered at V_F = (a) 0.03 and (b) $1.67\ K\ s^{-1}$ and $P_{pre} = 10$ MPa. White circles denote pores.

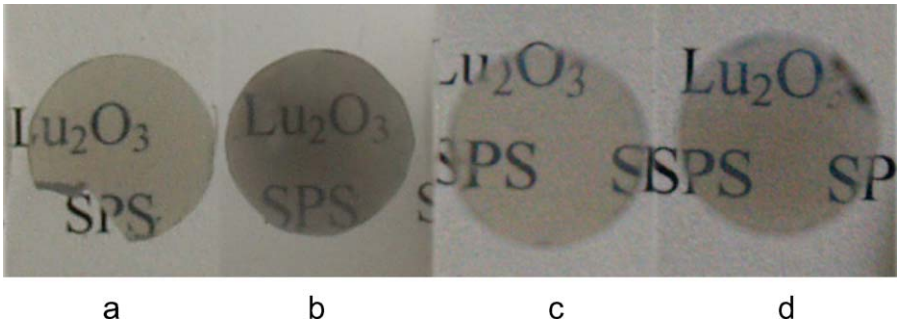

Fig. 8. Images of transparent Lu_2O_3 bodies sintered at different P_{pre} and V_F: (a) 10 MPa and 0.17 K s^{-1} (b) 100 MPa and 0.17 K s^{-1} (c) 10 MPa and 0.03 K s^{-1} and (d) 10 MPa and 1.67 K s^{-1}. Specimens are 30 mm above the printed text.

associating with grain growth, and thus the similar trend of sintering curves were observed almost independent of P_{pre} when a two-step pressure profile was used.[8]

Fig. 3 shows FESEM images of thermally etched and fracture surfaces of the Lu_2O_3 body sintered at P_{pre} = 10 and 100 MPa and V_F = 0.17 K s^{-1}. The grains exhibited equiaxed polyhedral shapes (Fig. 3a and b) and were smaller at P_{pre} = 100 MPa (Fig. 3b). Small pores around 100 nm in diameter were observed in both the fracture surfaces (white circles in Fig. 3c and d). The fracture mode was transgranular mixed with intergranular, independent of P_{pre}. Fig. 4 shows the effects of P_{pre} on the average grain size. The grain size decreased slightly from 0.77 to 0.65 μm, and the grain size distribution slightly narrowed with increasing P_{pre}. Chaim et al. also reported that significant particle coarsening occurred during the heating stage prior to the pressure application, resulting in larger grain sizes with wider distributions.[10] It indicates that the lower the P_{pre}, the more the particle coarsening in the initial stage of sintering. The large particles in the green compact (at the intermediate stage in which the final pressure was applied) might have caused the formation of larger grains and creation of a wider size distribution of the final body at lower P_{pre}.[10]

3.2. Effects of the heating rate

Fig. 5 shows the sintering curves of the Lu_2O_3 bodies at P_{pre} = 10 MPa and V_F = 0.03 to 1.67 K s^{-1} after the application of the final pressure (100 MPa). The relative density increased significantly after the application of the final pressure. The relative density also increased significantly at a high V_F.

Fig. 6 shows FESEM images of the fracture surfaces of the Lu_2O_3 body sintered at V_F = 0.03 and 1.67 K s^{-1} and P_{pre} = 10 MPa. Although all the specimens were nearly full dense at the end of sintering as shown in Fig. 5, pores can be observed located at the triple junctions of grain boundaries, and their number increased at higher V_F (Fig. 6b). Fig. 7 shows the effects of V_F on the average grain size. The average grain size slightly increased from 0.67 to 0.86 μm as V_F was increased from 0.03 to 1.67 K s^{-1}. The size distribution was almost the same, independent of V_F. Shen et al.[11] and Jiang et al.[12] reported that the grain size of Al_2O_3 bodies prepared by SPS decreased with increasing V_F. Olevsky et al.[13] presented a model based on grain boundary diffusion and creep densification to explain the smaller grain growth of Al alloy powder during SPS at higher V_F. In contrast, Chaim et al. reported the opposite trend in the grain size of a Y_2O_3 body by SPS.[14] Murayama et al. reported that for Al_2O_3, the grain growth rate at a high V_F (8.33 K s^{-1}) was greater than that at a low V_F (0.08 K s^{-1}) in hot pressing.[15] Kim et al. also reported that the grain size of Al_2O_3 sintered by SPS at 1423 K increased from 0.29 to 0.55 μm by increasing V_F from 0.17 to 1.67 K s^{-1}.[16] This trend was in agreement with the present results. As V_F increased, densification also increased promptly as shown in Fig. 5. More significant stress formation among the grains might have resulted in a larger average size at higher V_F.[17]

3.3. Transparency

Fig. 8 shows the photographs of transparent Lu_2O_3 sintered at different P_{pre} and V_F. The printed texts 30 mm below the specimens were readable, exhibiting high transparency. All the specimens were slightly gray in color. The color became darker at higher P_{pre} (100 MPa) and V_F values (1.67 K s^{-1}).

Fig. 9 shows the transmittance (T) spectra of Lu_2O_3 bodies sintered at V_F = 0.17 K s^{-1}. The transmittance showed a maximum value at P_{pre} = 30 MPa. Fig. 10 depicts the effects of P_{pre} on transmittances at wavelengths (λ) of 550 and 2000 nm. The transmittances at λ = 550 and 2000 nm showed maxima at 30 MPa, and the highest transmittances were 60% at λ = 550 nm and 79% at λ = 2000 nm. The transmittance in the infrared range

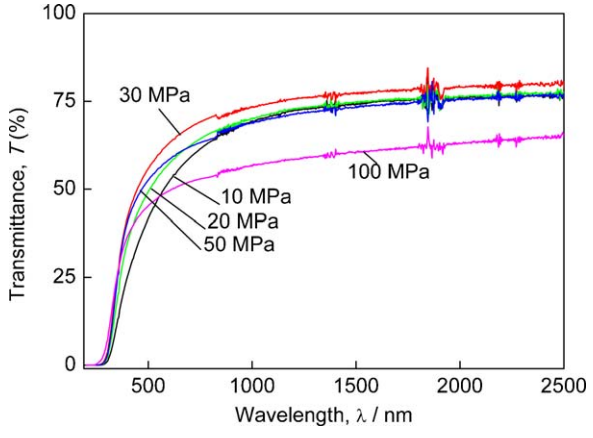

Fig. 9. Transmittance spectra of Lu_2O_3 bodies sintered at V_F = 0.17 K s^{-1}.

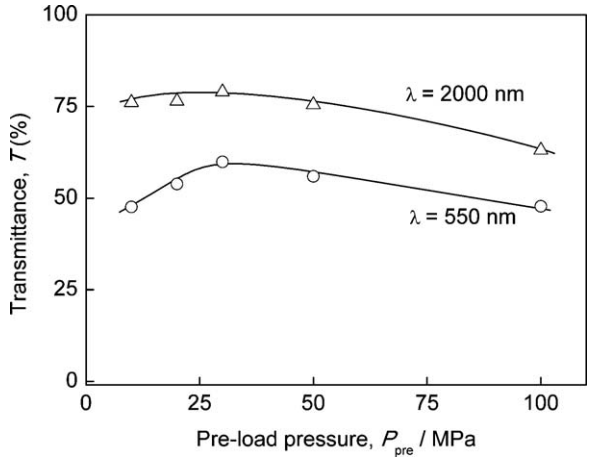

Fig. 10. Effect of P_{pre} on transmittance at wavelengths of 550 and 2000 nm.

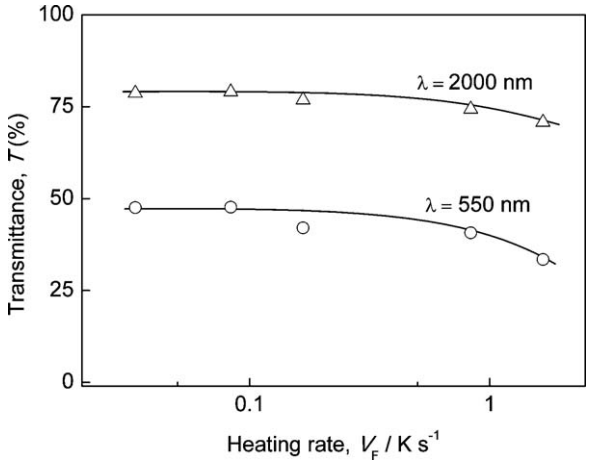

Fig. 12. Effect of V_F on transmittance at wavelengths of 550 and 2000 nm.

was greater than 75% and was almost independent of P_{pre}, while that in the visible range depended on P_{pre}. Pores of approximately 100 nm in diameter were identified at the grain boundaries as shown in Figs. 3c and d, which might have acted as scattering sources. Mie scattering by residual pores smaller than 100 nm in diameter would not affect the transmittance at $\lambda > 1000$ nm but could be detrimental in the visible range. Because of the reflective losses of both surfaces of the specimens, the theoretical transmittance is calculated as 82.5% at $\lambda = 2000$ nm.[18] Thus, the transmittances were 73 and 96% of the theoretical values at $\lambda = 550$ and 2000 nm, respectively. The present transmittance value at 550 nm was 20% lower than that prepared by a vacuum sintering technique,[18] but was 3% higher than that of an undoped Lu_2O_3 polycrystalline ceramic prepared in H_2 atmosphere[19] by comparing normalized thickness of 1.0 mm.

Fig. 11 shows the transmittance spectra of Lu_2O_3 bodies sintered at $P_{pre} = 10$ MPa and various V_F values. The transmittance increased with decreasing V_F. The transmittances increased from 40% to 54% at $\lambda = 550$ nm and from 70% to 79% at $\lambda = 2000$ nm as V_F decreased from 1.67 to 0.08 K s^{-1} (Fig. 12). As V_F was further decreased from 0.08 to 0.03 K s^{-1}, almost no change in the transmittance was observed.

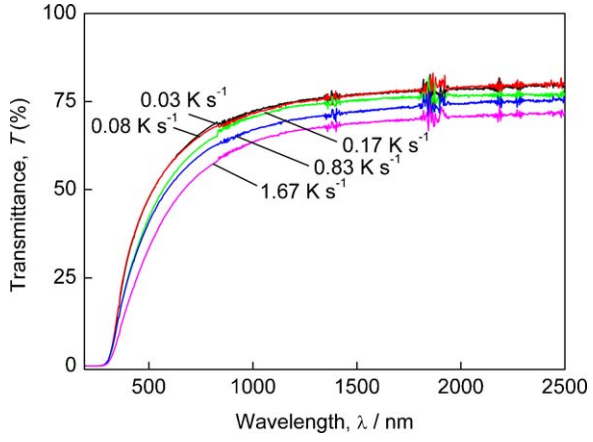

Fig. 11. Transmittance spectra of Lu_2O_3 bodies sintered at $P_{pre} = 10$ MPa.

ZrO_2,[20] Al_2O_3[3] and $MgAl_2O_4$[2,4] bodies sintered by SPS commonly exhibit a gray color. It is widely understood that defects, mainly oxide vacancies, can form during SPS because of the reduced atmosphere. As shown in Fig. 8, the color of the specimen sintered at $V_F = 1.67$ K s^{-1} was slightly darker than that at $V_F = 0.03$ K s^{-1}, suggesting a higher defect concentration introduced at higher V_F.[2] Defects would act as a source of light absorption or scattering over a wide wavelength range.[2,20] On the other hand, the pores observed in the fracture surfaces were another source of light scattering, as shown in Fig. 6. The large grain size often contains relatively large pores at the triple junctions. Morita et al. also reported that a high V_F enhanced the formation of closed pores and a wide pore distribution during SPS.[4] Because SPS is a short-time sintering process, the pores cannot have enough time to diffuse out through the grain boundaries. Defects, mainly oxide vacancies and pores, might have caused the decrease in the transmittance. The pre-load pressure could have a positive effect on destruction of agglomerates in the initial stage of sintering and suppression of particle coarsening prior to final pressure application. However, a high pre-load pressure would cause high defect concentration.[2] Therefore, a moderate pre-load pressure of 30 MPa was an optimal value in the present study. Highest transmittance was observed at this pre-load pressure.

4. Conclusions

Transparent Lu_2O_3 body was produced by SPS using a two-step pressure profile combined with a low heating rate. At $P_{pre} = 30$ MPa and $V_F = 0.17$ K s^{-1}, high transmittances of 60% and 79% at the wavelengths of 550 and 2000 nm were obtained, respectively. A high V_F resulted in a significant increase in relative density and a large grain size with an increasing number of pores, which degraded transparency. P_{pre} affected the intermediate relative density, and P_{pre} at 30 MPa led to the highest transparency. The transmittance in the visible range was more sensitive to P_{pre} than that in the infrared range. The combination of the low heating rate and the two-step pressure resulted

in a high transparency by inhibiting the defect formation and eliminating the pores.

Acknowledgments

This research was supported in part by the Research Fellowships of the Japan Society for the Promotion of Science for Young Scientists. This research was also supported in part by the Global COE Program of the Materials Integration, Tohoku University.

References

1. Munir ZA, Anselmi-Tamburini U, Ohyanagi M. The effect of electric field and pressure on the synthesis and consolidation of materials: a review of the spark plasma sintering method. *J Mater Sci* 2006;**41**:763–77.
2. Wang C, Zhao Z. Transparent $MgAl_2O_4$ ceramic produced by spark plasma sintering. *Scr Mater* 2009;**61**:193–6.
3. Kim B-N, Hiraga K, Morita K, Yoshida H. Spark plasma sintering of transparent alumina. *Scr Mater* 2007;**57**:607–10.
4. Morita K, Kim B-N, Yoshida H, Hiraga K. Spark-plasma-sintering condition optimization for producing transparent $MgAl_2O_4$ spinel polycrystal. *J Am Ceram Soc* 2009;**92**:1208–16.
5. Ikesue A, Aung YL. Ceramic laser materials. *Nat Photonics* 2008;**2**:721–7.
6. An LQ, Ito A, Goto T. Fabrication of transparent lutetium oxide by spark plasma sintering. *J Am Ceram Soc* 2011;**94**:695–8.
7. Mendelson MI. Average grain size in polycrystalline ceramics. *J Am Ceram Soc* 1969;**52**:443–6.
8. Chaim R, Levin M, Shlayer A, Estournes C. Sintering and densification of. nanocrystalline ceramic oxide powders: a review. *Adv Appl Ceram* 2008;**107**:159–69.
9. Ehre D, Gutmanas EY, Chaim R. Densification of nanocrystalline MgO ceramics by hot-pressing. *J Eur Ceram Soc* 2005;**25**:3579–85.
10. Chaim R, Shen ZJ. Grain size control by pressure application regime during spark plasma sintering of Nd-YAG nanopowders. *J Mater Sci* 2008;**43**:5023–7.
11. Shen ZJ, Johnsson M, Zhao Z, Nygren M. Spark plasma sintering of alumina. *J Am Ceram Soc* 2002;**85**:1921–7.
12. Jiang DT, Hulbert DM, Anselmi-Tamburini U, Ng T, Land D, Mukherjee AK. Optically transparent polycrystalline Al_2O_3 produced by spark plasma sintering. *J Am Ceram Soc* 2008;**91**:151–4.
13. Olevsky EA, Kandukuri S, Froyen L. Consolidation enhancement in spark-plasma sintering: impact of high heating rates. *J Appl Phys* 2007;**102**:114913.
14. Chaim R, Shlayer A, Estournes C. Densification of nanocrystalline Y_2O_3 ceramic powder by spark plasma sintering. *J Eur Ceram Soc* 2009;**29**:91–8.
15. Murayama N, Shin W. Effect of rapid heating on densification and grain growth in hot pressed alumina. *J Ceram Soc Jpn* 2000;**108**: 799–807.
16. Kim B-N, Hiraga K, Morita K, Yoshida H. Effects of heating rate on microstructure and transparency of spark-plasma-sintered alumina. *J Eur Ceram Soc* 2009;**29**:323–7.
17. Li C-W, Lui S-C, Goldacker J. Relation between strength, microstructure, and grain-bridging characteristics in *In Situ* reinforced silicon nitride. *J Am Ceram Soc* 1995;**78**:449–59.
18. Kaminskii AA, Akchurin MS, Becker P, Ueda K, Bohatý L, Shirakawa A, et al. Mechanical and optical properties of Lu_2O_3 host-ceramics for Ln^{3+} lasants. *Laser Phys Lett* 2008;**5**:300–3.
19. Zhou D, Shi Y, Xie JJ, Ren YY, Yun P. Fabrication and luminescent properties of Nd^{3+}-Doped Lu_2O_3 transparent ceramics by pressureless sintering. *J Am Ceram Soc* 2009;**92**:2182–7.
20. Anselmi-Tamburini U, Woolman JN, Munir ZA. Transparent nanometric cubic and tetragonal zirconia obtained by high-pressure pulsed electric current sintering. *Adv Funct Mater* 2007;**17**:3267–73.